A&A manuscript no.
(will be inserted by hand later)

Your thesaurus codes are:
08(08.16.5; 08.02.6; 13.09.6; 04.19.1; 03.20.2)

ASTRONOMY AND ASTROPHYSICS

Multiplicity of T Tauri Stars in Taurus after ROSAT

Rainer Köhler and Christoph Leinert

Max-Planck-Institut für Astronomie, Königstuhl 17, D-69117 Heidelberg, Germany

Received 1 September 1997, accepted 12 November 1997

Abstract. We surveyed a sample of 75 T Tauri stars in the Taurus star forming region for companions. These stars were discovered with the help of ROSAT. The separation range covered is $0.13''$ to $13''$, where the lower limit is given by the diffraction limit of the telescope and the upper limit by confusion with background stars. Combined with the results of the preceding survey by Leinert et al. (1993), we now have surveyed a sample of 178 young stars in Taurus, 63 classical, 106 weak-line, and 9 unclassified T Tauri stars. Within this sample, we find 68 binaries, 9 triples, and 3 quadruples. After corrections to account for confusion with background stars and for a bias induced through X-ray selection, we count 74 binaries or multiples with a total of 85 companions in 174 systems. This corresponds to a degree of multiplicity (number of binaries or multiples divided by number of systems) of $(42.5 \pm 4.9)\,\%$, or to a duplicity, measured by the number of companions per system, of $(48.9 \pm 5.3)\,\%$, which is higher by a factor of (1.93 ± 0.26) compared to solar-type main-sequence stars. We find no difference in duplicity between classical and weak-line T Tauri stars. There is a difference between close and wide pairs in the sense that close pairs have a flat distribution of flux ratios, while the flux ratios of wide pairs are peaked towards small values.

Key words: stars: pre-main-sequence – binaries: visual – infrared: stars – surveys – techniques: interferometric

1. Introduction

The announcement by Ghez et al. (1993) and Leinert et al. (1993) that almost all young stars in the Taurus and Ophiuchus star forming regions might be binaries came as a surprise. Their results were sufficiently different from those obtained for the main sequence (Duquennoy and Mayor 1991, DM91) to suggest that a strong evolution of binarity was required during later stages of the pre-main-sequence phase. It is not easy to explain these changes in the binarity on relatively short timescales. However, as stated by e. g. Ghez et al. (1997), there are several other possibilities which do not require this evolution in binarity.

For example, the Taurus and Ophiuchus samples studied by the above authors may not be representative because they mainly contain classical T Tauri stars (showing strong Hα line emission). According to the ROSAT survey, however, the majority of young stars are X-ray emitting weak-line T Tauri stars. From EINSTEIN observations of 20 % of the area of the Taurus-Auriga star forming region, Walter et al. (1988) already had extrapolated a WTTS/CTTS ratio of 10. With the help of the ROSAT All-Sky Survey (RASS), Wichmann et al. (1996) found a lower limit of about 6 for this ratio, while the findings of Neuhäuser et al. (1995) arrived at a ratio of 8.

Another possibility why the multiplicity surveys mentioned above may not be representative is because the associations in Taurus and Ophiuchus are not typical locations for star formation. Miller & Scalo (1978) report that 75 % of present-day star formation occur in OB associations and newer studies suggest that a significant fraction of all stars formed in the galaxy begin their lives in rich embedded clusters (Lada & Lada 1991, Kroupa 1995). For example, Petr et al. (1998) measure a binary proportion in the Trapezium cluster core that is similar to that in the Galactic field (see also Prosser et al. 1994).

In this paper we test the first of these two hypotheses by observing the X-ray selected WTTS in Taurus, which are representative of the majority of the young stars, and checking for multiplicity. It is natural to begin such a comparison in Taurus since the duplicity survey on the CTTS in this region carries the best statistical weight.

2. The sample

This work is based on the results of Wichmann et al. (1996), who searched for hitherto undiscovered T Tauri

Send offprint requests to: Rainer Köhler
Correspondence to: koehler@mpia-hd.mpg.de

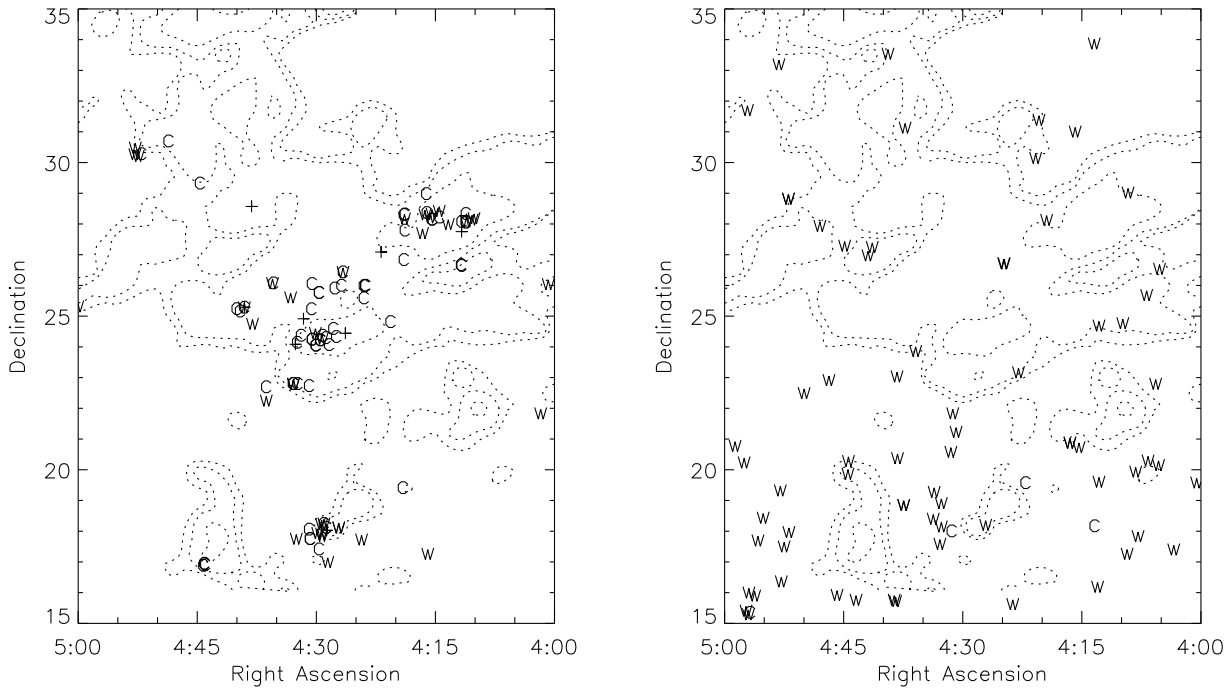

Fig. 1. Spatial distribution of T Tauri stars known prior to ROSAT (left panel) and the new T Tauri stars discovered by Wichmann et al. (1996, right panel). Our combined sample consists of the stars in the left plus the stars in the right panel. Classical T Tauri stars are marked by "C", weak-line T Tauri stars by "W", and unclassified T Tauri stars by crosses. The dotted contours represent the integrated CO J=1–0 line brightness (Ungerechts & Thadeus 1987)

stars on the basis of the ROSAT All-Sky Survey and additional pointed ROSAT observations. Their identification of ROSAT sources by means of optical spectroscopy revealed a total of 76 new T Tauri stars in the Taurus region, located between 4^h and 5^h in right ascension and between 15° and 34° in declination. 68 of these sources are in the All-Sky Survey, the remaining 8 were found with pointed observations. 72 were classified as weak-line T Tauri stars (WTTS) based on an equivalent width of the Hα emission line $W_\lambda(H\alpha) \leq 10$ Å, 4 as classical T Tauri star (CTTS). The complete object list can be found in Wichmann et al. (1996).

One star of this sample (RXJ0422.9+2310) turned out to be too faint for speckle observations. We observed it in October 1995 and September 1996 and were forced to use an integration time of 3 seconds to obtain a signal of only a few hundred counts. This is much too long for speckle imaging, so we decided to exclude this star from our survey. Two other stars (RXJ0437.4+1851A and B) are only 4" separated from each other, so we count them as one binary. Therefore, we start our survey with a sample of 74 systems, where "system" means either a single star, a binary, or a multiple.

This sample supplements the work of Leinert et al. (1993), who surveyed all the young stars contained in the Herbig-Bell catalogue which are located in the same region and are brighter than K = 9.5 mag, i. e. the T Tauri stars known before ROSAT. Their sample contained 104 systems, 59 classical, 36 weak-line, and 9 unclassified T Tauri stars. The spatial distribution of both samples is shown in Fig. 1. It is obvious from this figure that the TTS known before ROSAT cluster on the CO maxima, while the ROSAT-discovered sources do not and thus probably represent an independent population.

3. Observations

We are searching for companions with separations in the two decades from 0.13″ to 13″ to include the separation where the distribution of main sequence binaries has its maximum ($\approx$ 40 AU, $\approx$ 0.3″ at the distance of Taurus). The lower limit is determined by the theoretical diffraction limit of the 3.5 m telescope on Calar Alto at a wavelength of 2.2 μm. The upper limit is chosen so that the contamination by background stars has little effect (for a detailed discussion of this problem see Sect. 4.2). To make maximum use of the resolution of the 3.5 m telescope, the main observational technique for our survey is speckle interferometry, complemented by direct imaging to find companions that are outside the limited field of view of today's speckle cameras.

The speckle observations were carried out at the 3.5 m telescope on Calar Alto in September 1994, December

Table 1. New binary WTTS in Taurus. The first column gives the number of the star as in Table 4 of Wichmann et al. (1996); the second gives the official designation; the third column specifies to which pair of a higher-order multiple system the following parameters apply; the fourth column gives the total system brightness in K. The following columns contain the date of the observation and the position and brightness of the companion relative to the primary (i. e. the star brighter in K). For a description of the way the errors were determined see text. If a companion was observed more than once, the different observations are listed in separate rows. Stars marked with [p] were found with pointed ROSAT observations

No.	Designation		m_K [mag]	Date of Observation	Separation ["]	Position Angle [°]	Brightness Ratio at K
1	HD 285281		7.61 ± 0.01	12. Dec. 94	0.773 ± 0.003	190.7 ± 0.4	0.323 ± 0.010
5	HD 284135		7.75 ± 0.01	15. Sep. 94	0.378 ± 0.003	75.2 ± 0.5	0.822 ± 0.019
7	RXJ0406.8+2541		7.75 ± 0.01	15. Sep. 94	0.977 ± 0.019	12.3 ± 1.2	0.964 ± 0.024
10	RXJ0409.1+2901		8.12 ± 0.01	2. Jan. 96	6.786 ± 0.006	138.7 ± 1.0	0.231 ± 0.001
				3. Mar. 96	6.764 ± 0.025	138.9 ± 0.2	0.245 ± 0.012
13	RXJ0412.8+1937		9.03 ± 0.01	12. Dec. 94	2.568 ± 0.004	35.3 ± 0.4	0.379 ± 0.014
17	RXJ0413.4+3352		9.96 ± 0.05	8. Oct. 95	1.008 ± 0.003	247.9 ± 0.1	0.056 ± 0.004
18	RXJ0415.3+2044		8.60 ± 0.01	12. Dec. 94	0.589 ± 0.003	356.8 ± 0.4	0.170 ± 0.009
19	RXJ0415.8+3100		9.92 ± 0.01	16. Sep. 94	0.940 ± 0.003	147.2 ± 0.5	0.264 ± 0.006
24	RXJ0420.8+3009	A-B	10.35 ± 0.01	16. Sep. 94	0.189 ± 0.009	342.4 ± 1.2	0.622 ± 0.077
		AB-C		21. Jan. 95	6.648 ± 0.013	59.3 ± 0.1	0.201 ± 0.003
		AB-C		24. Nov. 96	6.693 ± 0.032	59.6 ± 0.7	0.242 ± 0.014
25	RXJ0422.1+1934[p]		8.75 ± 0.03	2. Feb. 96	11.758 ± 0.057	316.8 ± 0.1	0.057 ± 0.006
29	BD+26 718B	A-a	7.39 ± 0.01	16. Sep. 94	0.496 ± 0.003	320.1 ± 0.5	0.148 ± 0.016
		A-a		27. Sep. 96	0.474 ± 0.003	320.0 ± 0.1	0.147 ± 0.011
		A-B		16. Sep. 94	7.872 ± 0.071	158.7 ± 0.9	0.452 ± 0.005
		A-B		24. Nov. 96	7.936 ± 0.045	158.4 ± 0.1	0.488 ± 0.002
		B-b		16. Sep. 94	0.166 ± 0.007	136.8 ± 9.0	0.510 ± 0.090
		B-b		27. Sep. 96	0.155 ± 0.003	133.4 ± 0.2	0.612 ± 0.029
30	BD+17 724B		7.82 ± 0.01	8. Oct. 95	0.100 ± 0.011	208.7 ± 9.7	0.123 ± 0.022
				27. Sep. 96	0.083 ± 0.003	193.5 ± 2.1	0.240 ± 0.018
31	RXJ0430.8+2113		8.39 ± 0.01	14. Dec. 94	0.389 ± 0.013	151.5 ± 2.0	0.037 ± 0.013
32	HD 284496		8.71 ± 0.01	28. Feb. 96	4.598 ± 0.061	337.7 ± 1.4	0.020 ± 0.002
33	RXJ0431.3+1800[p]		10.47 ± 0.03	2. Feb. 96	10.423 ± 0.074	238.9 ± 0.5	0.075 ± 0.014
40	RXJ0435.9+2352	A-B	8.45 ± 0.02	17. Sep. 94	0.069 ± 0.003	166.8 ± 0.9	0.309 ± 0.015
		AB-C[†]		2. Feb. 96	11.315 ± 0.011	270.4 ± 0.1	0.170 ± 0.003
41	RXJ0437.2+3108		9.44 ± 0.01	17. Sep. 94	0.109 ± 0.003	16.3 ± 1.0	0.386 ± 0.009
42/43	RXJ0437.4+1851		8.05 ± 0.02	14. Dec. 94	4.345 ± 0.003	185.0 ± 0.4	0.680 ± 0.010
				24. Nov. 96	4.353 ± 0.038	184.7 ± 0.3	0.730 ± 0.010
44	RXJ0438.2+2023		9.36 ± 0.01	14. Dec. 94	0.464 ± 0.003	352.4 ± 0.6	0.911 ± 0.032

1994, and October 1995. We used MAGIC, a 256×256 pixel NICMOS 3-camera (Herbst et al. 1993), at K = $2.2\,\mu$m in its high-resolution configuration at the f/45 focus. This gives a pixel scale of $0.0713''$/pixel and a field of view of $18.7'' \times 18.7''$. For our speckle observations, we usually use only one quarter of the array, unless we see a companion in the rest of the field. At each observing run, we measured a number of well-known binary stars to calibrate the pixel scale and position angle.

The modulus of the complex visibility (i. e. the Fourier transform of the object brightness distribution) is determined from power spectrum analysis, the phase is computed using the Knox-Thompson algorithm (Knox & Thompson 1974), and from the bispectrum (Lohmann 1983). If the object turns out to be a binary, we obtain the brightness ratio, separation and position angle of the components from a fit of binary models to the complex visibility. Fits to different subsets of the data give an estimate for the standard deviation of the binary parameters. This procedure sometimes yields unbelievable small errors, we estimate the minimal error of the separation to be about 1/20 pixel or $0.003''$, the minimal error of the position angle to be $0.1°$, and the minimal error of the brightness ratio to be 0.001. These might be slightly larger for the binaries with the smallest separations.

Otherwise, if the object appears to be unresolved, upper limits for the maximum brightness of an undetected companion are determined by computing the maximum brightness ratio of a companion that could be hidden in the noise of the data. For details of this procedure see Leinert et al. (1996).

The additional imaging has been done at different telescopes on Calar Alto, namely the 2.2 m telescope in January 1995, the 3.5 m telescope at the f/10 focus in January 1996, and the 1.23 m telescope in February 1996. Again, we used MAGIC at K = 2.2μm in its high-resolution configu-

Table 1. New binary WTTS in Taurus (continued)

No.	Designation		m_K [mag]	Date of Observation	Separation ["]	Position Angle [°]	Brightness Ratio at K
45	RXJ0438.2+2302		9.70 ± 0.03	2. Feb. 96	9.190 ± 0.057	93.3 ± 0.1	0.101 ± 0.013
47	HD 285957	A-B	8.02 ± 0.01	15. Dec. 94	9.463 ± 0.017	200.0 ± 0.4	0.184 ± 0.007
		A-B		24. Nov. 96	9.504 ± 0.064	199.0 ± 0.5	0.202 ± 0.012
		A-C		21. Jan. 95	10.345 ± 0.006	312.0 ± 0.1	0.013 ± 0.001
		A-C		24. Nov. 96	10.396 ± 0.045	312.9 ± 0.3	0.014 ± 0.001
49	RXJ0441.4+2715		10.32 ± 0.08	18. Sep. 94	0.065 ± 0.003	216.0 ± 1.7	0.558 ± 0.089
50	HD 283798	A-B	7.98 ± 0.01	18. Sep. 94	1.631 ± 0.003	303.1 ± 0.5	0.043 ± 0.005
		AB-C		29. Feb. 96	7.147 ± 0.067	64.2 ± 0.5	0.005 ± 0.002
52	RXJ0444.3+2017		9.18 ± 0.04	3. Mar. 96	9.868 ± 0.029	159.7 ± 0.1	0.105 ± 0.037
53	RXJ0444.4+1952	A-B	8.55 ± 0.01	14. Dec. 94	0.207 ± 0.003	158.1 ± 0.7	0.927 ± 0.034
		AB-C		3. Feb. 96	6.078 ± 0.045	96.3 ± 0.6	0.206 ± 0.043
		AB-C		24. Nov. 96	6.113 ± 0.025	97.2 ± 0.3	0.156 ± 0.003
54	RXJ0444.9+2717		7.19 ± 0.01	18. Sep. 94	1.754 ± 0.003	48.1 ± 0.5	0.102 ± 0.001
55	HD 30171		7.16 ± 0.01	21. Jan. 95	12.926 ± 0.064	175.8 ± 0.1	0.207 ± 0.001
57	RXJ0447.9+2755		9.52 ± 0.01	18. Sep. 94	0.639 ± 0.003	86.5 ± 0.5	0.895 ± 0.024
58	RXJ0450.0+2230	A-B	8.86 ± 0.02	14. Dec. 94	2.072 ± 0.004	84.1 ± 0.4	0.032 ± 0.001
		AB-C		2. Feb. 96	8.361 ± 0.091	296.1 ± 0.4	0.033 ± 0.013
59	RXJ0451.8+1758		9.26 ± 0.01	14. Dec. 94	0.568 ± 0.003	344.8 ± 0.4	0.756 ± 0.023
60	RXJ0451.9+2849A		9.88 ± 0.01	21. Jan. 95	7.636 ± 0.025	106.7 ± 0.3	0.025 ± 0.002
61	RXJ0451.9+2849B		11.25 ± 0.01	12. Dec. 94	0.287 ± 0.006	321.4 ± 2.7	0.80 ± 0.10
63	RXJ0452.8+1621		8.25 ± 0.01	15. Dec. 94	0.478 ± 0.003	294.7 ± 0.4	0.837 ± 0.041
64	RXJ0452.9+1920		9.17 ± 0.01	14. Dec. 94	0.425 ± 0.003	304.5 ± 0.6	0.182 ± 0.022
65	RXJ0453.1+3311	A-B	10.86 ± 0.01	13. Dec. 94	0.687 ± 0.003	340.5 ± 0.4	0.649 ± 0.048
		AB-C		21. Jan. 95	7.834 ± 0.019	300.5 ± 0.1	0.335 ± 0.007
		AB-C		24. Nov. 96	7.853 ± 0.032	300.8 ± 0.3	0.347 ± 0.008
67	RXJ0455.7+1742		8.97 ± 0.03	15. Dec. 94	0.093 ± 0.003	254.6 ± 1.4	0.684 ± 0.052
69	RXJ0456.7+1521		10.61 ± 0.02	14. Dec. 94	0.160 ± 0.003	349.1 ± 0.7	0.800 ± 0.034
71	HD 286179		8.48 ± 0.02	15. Dec. 94	0.112 ± 0.003	208.3 ± 1.3	0.313 ± 0.023
73	RXJ0457.2+1524		7.78 ± 0.01	15. Dec. 94	0.570 ± 0.003	43.9 ± 0.4	0.955 ± 0.020
74	RXJ0457.5+2014		8.61 ± 0.01	14. Dec. 94	6.867 ± 0.006	205.5 ± 0.4	0.108 ± 0.005
				24. Nov. 96	6.865 ± 0.057	204.8 ± 0.2	0.132 ± 0.002
75	RXJ0458.7+2046		8.80 ± 0.02	14. Dec. 94	6.113 ± 0.014	220.4 ± 0.4	0.002 ± 0.001

†: The spectrum of star No. 40C shows no Lithium line, this object is probably a background star (R. Wichmann, priv. comm.). The m_K given for star 40 is the magnitude *without* component C

ration. The pixel scales were 0.66″/pixel at the 2.2 m telescope, 0.32″/pixel at the 3.5 m telescope, and 1.2″/pixel at the 1.23 m telescope. Some images were taken at the 2.2 m telescope on La Silla in March 1996, using the IRAC2b camera (another 256 × 256 pixel NICMOS-3 array) with its objective "B", which gives a pixel scale of 0.27″/pixel. Some of the imaging observations could also be used to obtain infrared photometry of the stars.

4. Results for the X-ray selected sample

4.1. Uncorrected data

Table 1 lists all the binary and multiple stars we find in our sample. Table 2 lists all stars where we did not find a companion and gives limits for the brightness of an undetected companion. Figure 2 shows the results in a plot of flux ratio and magnitude difference vs. binary star separation. In total, we find 29 binary, 6 triple and 1 quadruple star with separations in the range between 0.13″ and 13″.

The lower separation limit is the diffraction limit of the 3.5 m telescope at K for binary stars. In principle, it is possible to discover binaries with even smaller separations (Table 1 shows that we actually do find some). However, we cannot distinguish with certainty a close binary star below the diffraction limit from an elongated structure.

The upper limit was chosen so that contamination with background stars has little effect (see the following section for a detailed discussion of this problem). Leinert et al. (1993) chose the same value of 13″ in their survey.

Figure 2 also shows the sensitivity of our survey, i. e. the maximum brightness ratio of a possible undetected companion as a function of the separation. On average our survey is sensitive to companions brighter than 6 % of the primary for all separations larger than 0.13″. *All* observations are sensitive to companions brighter than 18 %. Based on the curves for individual observations and the

Table 2. Unresolved stars in our sample and limits for undetected companions. Objects marked with [p] were found with pointed ROSAT observations

No.	Designation	m_K [mag]	Date of Observation	Maximum Flux Ratio at 0.13″	Maximum Flux Ratio at 0.5″	Minimal Δm_K [mag] at 0.13″	Minimal Δm_K [mag] at 0.5″
2	RXJ0403.3+1725	8.77 ± 0.01	13. Dez. 94	0.04	0.03	3.49	3.81
3	RXJ0405.1+2632	9.27 ± 0.02	15. Sep. 94	0.1	0.06	2.50	3.05
4	RXJ0405.3+2009	8.14 ± 0.02	12. Dez. 94	0.08	0.04	2.74	3.49
6	HD 284149	8.10 ± 0.01	12. Dez. 94	0.06	0.02	3.05	4.25
8	RXJ0407.8+1750	8.96 ± 0.01	13. Dez. 94	0.07	0.02	2.89	4.25
9	RXJ0408.2+1956	9.44 ± 0.03	12. Dez. 94	0.1	0.05	2.50	3.25
11	RXJ0409.2+1716	9.12 ± 0.01	13. Dez. 94	0.07	0.04	2.89	3.49
12	RXJ0409.8+2446	9.25 ± 0.02	15. Sep. 94	0.13	0.04	2.22	3.49
14	RXJ0412.8+2442	8.85 ± 0.01	16. Sep. 94	0.13	0.07	2.22	2.89
15	HD 285579	11.24 ± 0.04	13. Dez. 94	0.07	0.06	2.89	3.05
16	RXJ0413.3+1810	10.48 ± 0.10	13. Dez. 94	0.08	0.05	2.74	3.25
20	RXJ0416.5+2053A[p]	10.08 ± 0.01	12. Dez. 94	0.17	0.08	1.92	2.74
21	RXJ0416.5+2053B[p]	11.11 ± 0.01	12. Dez. 94	0.18	0.09	1.86	2.61
22	RXJ0419.4+2808[p]	8.94 ± 0.02	16. Sep. 94	0.03	0.06	3.81	3.05
23	RXJ0420.3+3123	9.69 ± 0.01	16. Sep. 94	0.06	0.02	3.05	4.25
27	HD 285751	8.83 ± 0.02	17. Aug. 95	0.09	0.10	2.61	2.50
28	BD+26 718	7.61 ± 0.01	16. Sep. 94	0.05	0.03	3.25	3.81
34	RXJ0431.4+2035	10.12 ± 0.03	14. Dez. 94	0.06	0.02	3.05	4.25
35	RXJ0432.6+1809[p]	10.41 ± 0.04	13. Dez. 94	0.08	0.06	2.74	3.05
36	RXJ0432.7+1853[p]	8.64 ± 0.01	14. Dez. 94	0.05	0.03	3.25	3.81
37	RXJ0432.8+1735[p]	8.93 ± 0.01	13. Dez. 94	0.08	0.05	2.74	3.25
38	RXJ0433.5+1916	10.24 ± 0.06	12. Dez. 94	0.04	0.01	3.49	5.00
39	RXJ0433.7+1823	9.21 ± 0.06	13. Dez. 94	0.05	0.01	3.25	5.00
46	RXJ0438.4+1543	10.09 ± 0.02	13. Dez. 94	0.03	0.04	3.81	3.49
48	RXJ0439.4+3332A	8.44 ± 0.01	18. Sep. 94	0.05	0.04	3.25	3.49
51	RXJ0443.4+1546	9.83 ± 0.06	13. Dez. 94	0.045	0.03	3.37	3.81
56	RXJ0446.8+2255	9.02 ± 0.03	14. Dez. 94	0.025	0.02	4.01	4.25
62	RXJ0452.5+1730	9.22 ± 0.01	15. Dez. 94	0.05	0.04	3.25	3.49
66	HD 31281	7.63 ± 0.01	15. Dez. 94	0.09	0.05	2.61	3.25
68	RXJ0456.2+1554	9.49 ± 0.01	15. Dez. 94	0.06	0.05	3.05	3.25
70	RXJ0457.0+1600	9.84 ± 0.02	14. Dez. 94	0.07	0.04	2.89	3.49
72	RXJ0457.0+3142	7.14 ± 0.14	14. Dez. 94	0.05	0.05	3.25	3.25
76	RXJ0459.7+1430	8.96 ± 0.01	14. Dez. 94	0.03	0.02	3.81	4.25

number of companions actually found, we expect about 0.14 additional companions above 10 % brightness ratio at separations $< 0.4''$. Thus, we are confident we have found all companions brighter than 10 % of their primary. This corresponds to a magnitude difference of 2.5 mag.

4.2. Confusion with background stars

We expect a certain number of our wide binaries to be no physically bound pairs, but appear to be binaries due to chance projections of background stars. To quantify this effect, we count the field stars in the 32 images taken at the 1.23 m telescope. We exclude a circular area with a radius of $15''$ around the T Tauri star in each image. The remaining area is 23.2 arcmin^2 per field, giving a total area of 742.8 arcmin^2. These are the same images as used in our search for companions, which ensures that we have exactly the same magnitude limit.

Figure 3 shows the results of this procedure. The measured distribution of field stars is approximately the same as a Poisson distribution with a mean of 9.5. This corresponds to a background star density of $(1.1 \pm 0.1) \cdot 10^{-4}$ stars per arcsec^2. Leinert et al. (1993) find $4 \cdot 10^{-5}$ stars brighter than 12^{mag} per arcsec^2. The difference is partly due to the different magnitude limit, and partly due to the different spatial distributions of the two samples: the stars of Leinert et al. (1993) are more concentrated towards the dark clouds where the extinction is higher and therefore less background stars are visible.

Given the background star density, we can calculate the expected number of background stars with a projected distance of at most $13''$ to one of our 74 T Tauri stars:

$$1.1 \cdot 10^{-4} \cdot \pi \cdot 13^2 \cdot 74 = 4.3 \; .$$

In other words: the probability for a background star with a projected distance of at most $13''$ to *one* object is 4.3/74 = 6 %.

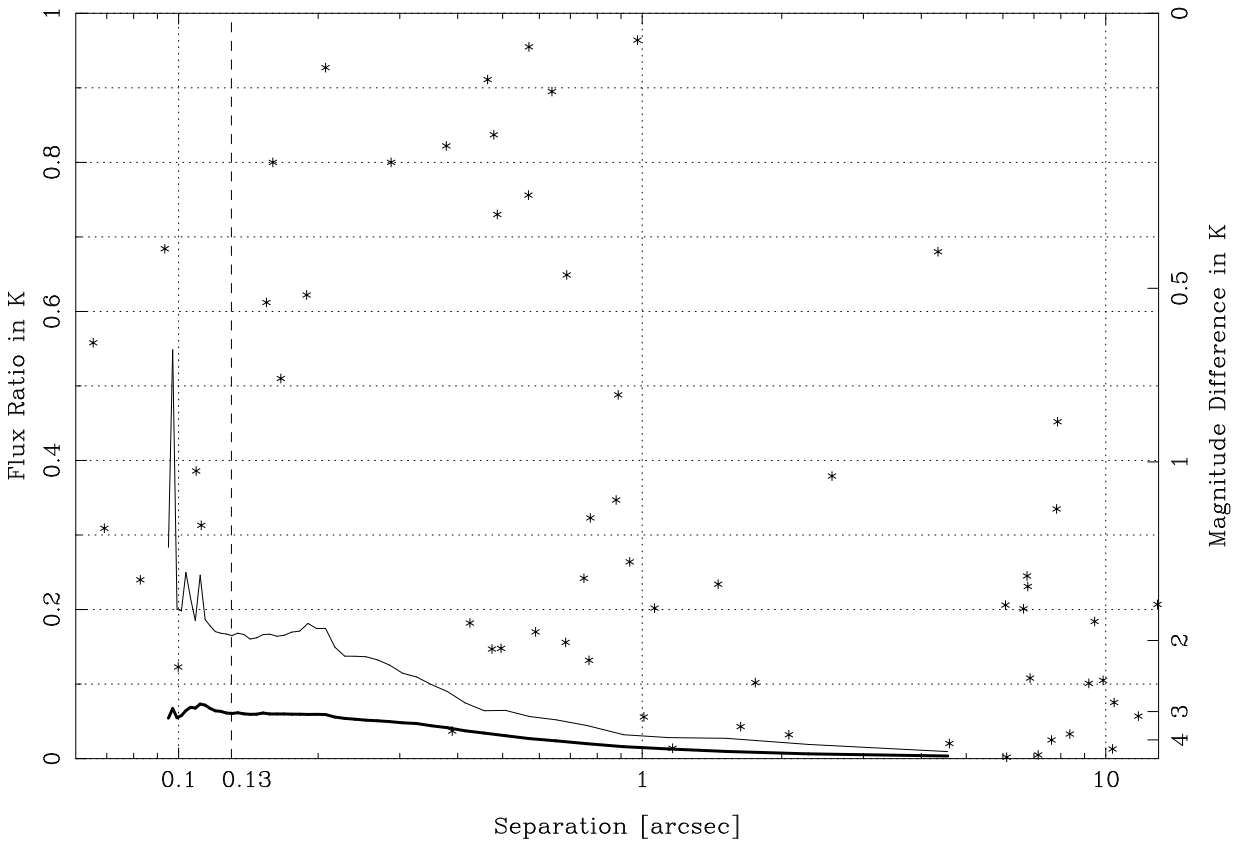

Fig. 2. The results of our multiplicity survey in a plot of flux ratio or magnitude difference vs. binary star separation. The thick line shows the average, the thin line the worst sensitivity for undetected companions. The dashed vertical line at 0.13″ shows the diffraction limit for a 3.5 m telescope at K. This is the limit for unambiguous identification of binaries stars. Each observation of a companion is marked individually, i. e. some companions occur more than once in this diagram

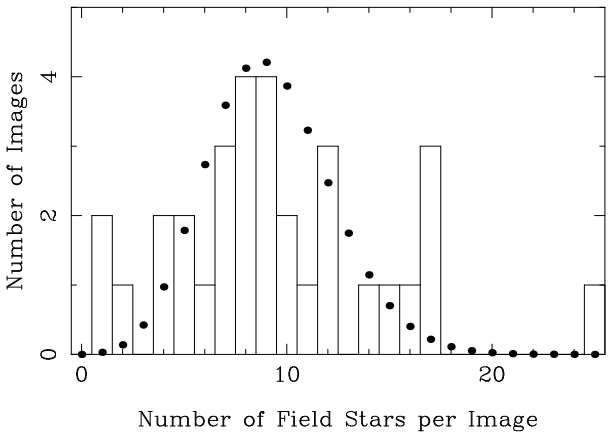

Fig. 3. Distribution of the number of field stars in 32 images. The histogram shows the number of background stars we count in our images; the dots denote a Poisson distribution with the same average star density

To estimate the number of physically bound companions, we have to subtract the number of chance projections from the total number of companions. This yields $44 - 4.3 \approx 40$ companions. To correct the numbers of binaries, triples, and quadruples, we have to take into account the relative numbers of single, binary, and triple stars (a binary caused by a nearby background object is in fact a single star, thus the number of "false" binaries depends on the number of single stars). This way, we arrive at about 2.4 binaries and 1.7 triple stars caused by chance projections. The corrected numbers of physically bound objects are consequently 29 binaries, 4 triples, and 1 quadruple star.

Unfortunately, we cannot say which companions are bound and which are chance projections. We do know, however, that the star 40C is one of the chance projections as Rainer Wichmann took a spectrum of it (priv. comm.). This spectrum shows no Lithium line, thus we know this star is no pre-main-sequence object. To identify further background stars it would be necessary to carry out additional spectroscopic observations.

4.3. Bias induced through X-ray selection

Brandner et al. (1996) pointed out that ROSAT-unresolved binaries are statistically brighter X-ray sources than single stars. Since the ROSAT All-Sky Survey is X-ray-flux limited, this induces a detection bias. Binaries with

component X-ray luminosities below, but combined luminosity above the cut-off, will cause an overestimate of the actual binary frequency.

The X-ray luminosities of our stars are known so we can check which binaries could have been detected only because of this bias. The worst case would be if all binaries consisted of two components with equal luminosities. Then all binaries with luminosity L_x between $L_{\rm limit}$ and $2L_{\rm limit}$ would have been detected only because of the detection bias.

In reality, only a small fraction of the binaries consist of two equally bright components. We would over-correct the bias if we excluded all binaries with $L_x < 2L_{\rm limit}$. We need an estimate for the number of binaries with both components below $L_{\rm limit}$. To obtain this, we start with the X-ray luminosity function given by Brandner et al. (1996). They used the X-ray luminosities of 47 Hα detected TTS associated with the dark cloud Chamaeleon I to derive the following relation:

$$\frac{{\rm d}N}{{\rm d}L_x} \propto L_x^{-1} \quad \text{for } 10^{21.5}\,{\rm W} < L_x < 10^{23.5}\,{\rm W}.$$

We use this as a reasonable approximation for the luminosity function of single stars.

We now consider a binary with total X-ray luminosity $L_{\rm tot}$ and component luminosities L_1 and L_2, where $L_1 \geq L_2$ and $L_1 + L_2 = L_{\rm tot}$. Therefore we have $L_1 \geq L_{\rm tot}/2$. The probability for both components to be fainter than $L_{\rm limit}$ is identical to the probability for the brighter component to be fainter than $L_{\rm limit}$:

$$\begin{aligned} P(L_1 < L_{\rm limit}) &\propto \int_{L_{\rm tot}/2}^{L_{\rm limit}} L_1^{-1}\,{\rm d}L_1 \\ &= \ln(L_{\rm limit}) - \ln(L_{\rm tot}/2)\,. \end{aligned}$$

We obtain the proportional constant by using the fact that $P = 1$ for $L_{\rm tot} = L_{\rm limit}$. Thus,

$$P = \frac{\log_{10}(L_{\rm limit}) - \log_{10}(L_{\rm tot}) + \log_{10} 2}{\log_{10} 2}\,.$$

This is a linear relationship between P and $\log(L_{\rm tot}) - \log(L_{\rm limit})$.

In this derivation, we assume that the probability for a second component with the correct L_2 is independent of L_2, i. e. we neglect the (unknown) distribution of X-ray flux ratios in binaries. This does not change the general trend, but it simplifies the calculation.

The probability that both components of a binary are fainter than $L_{\rm limit}$ is 33 % if $\log(L_{\rm tot}) = \log(L_{\rm limit}) + 0.2$. We decide to use this value of $L_{\rm tot}$ as borderline and to consider all fainter binaries as discovered because of the detection bias. This means we have to exclude them from our survey to obtain an unbiased sample.

It is possible to derive a relation for triple stars similar to Eq. (4) by replacing the factor 2 by 3. This yields a borderline for triples of $\log(L_{\rm tot}) \approx \log(L_{\rm limit}) + 0.32$.

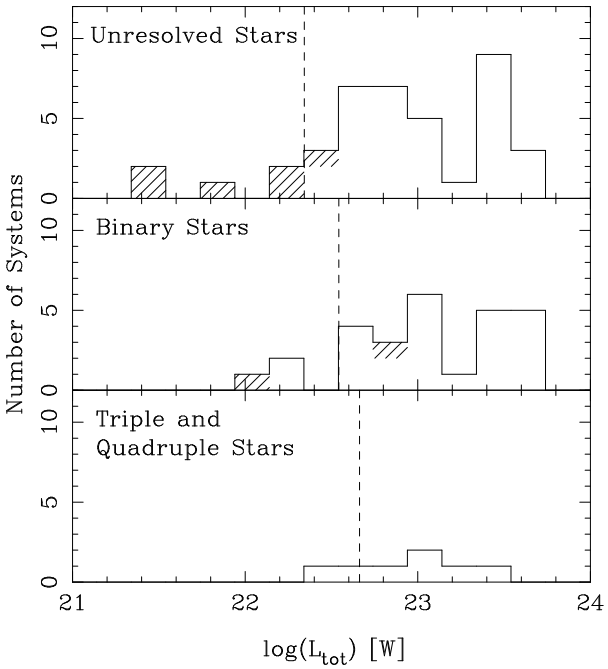

Fig. 4. X-ray luminosities of the T Tauri stars discovered by ROSAT, broken down into unresolved, binary, triple, and quadruple systems. Stars discovered with pointed ROSAT observations are hatched, all the others have been found with the All-Sky Survey. The vertical lines mark the luminosity limits chosen by us to obtain an unbiased sample: the luminosity limit of the RASS in Taurus-Auriga for unresolved stars ($2.2 \cdot 10^{22}$ W), $\log(L_{\rm limit}) + 0.2$ for binaries, and $\log(L_{\rm limit}) + 0.3$ for triple stars

Table 3. Binaries and triples we think have only been discovered because of the X-ray selection bias

No.	Designation		$\log(L_{\rm X})$[W]
24	RXJ0420.8+3009	triple	22.56
60	RXJ0451.9+2849A	binary	22.28
61	RXJ0451.9+2849B	binary	22.28
65	RXJ0453.1+3311	triple	22.49

Figure 4 shows the numbers of unresolved, binary, triple, and quadruple stars vs. their X-ray luminosities. The luminosity limit of the RASS in Taurus-Auriga, $L_{\rm limit} = 2.2 \cdot 10^{22}$ W (Wichmann et al. 1996), and the corresponding limits for binaries and triples are also shown. In a few cases ROSAT could measure only the combined X-ray flux of two stars due to its limited spatial resolution. However, they are too far apart from each other to be considered a binary. Therefore, we assign half of the combined flux to each star in these cases.

The upper panel of Fig. 4 clearly shows that one of the binaries and all of the unresolved stars fainter than the limiting luminosity of the RASS have been discovered in pointed observations. However, there are two binary and two triple stars from the all-sky survey below their

Table 4. Comparison of multiplicity in the ROSAT-selected Taurus sample and in the sample studied by Leinert et al. (1993)

	Sample size	Percentage of			
		Unresolved Stars	Binaries	Triples	Quadruples
Leinert et al. (1993)	104 stars	57.7 %	37.5 %	2.9 %	1.9 %
This Work	70 stars	57.1 %	38.6 %	2.9 %	1.4 %

corresponding limit. Table 3 lists the names and X-ray luminosities of these four stars.

To correct the X-ray selection bias, we have to subtract six companions from the result derived in Sect. 4.2. Furthermore, we have to subtract four from the total number of systems, since these stars have been detected only because their combined luminosity is above the limit. This yields a corrected sample with 70 systems, 27 binaries, 2 triples, and 1 quadruple star, giving a total of 34 companions. This corresponds to (49 ± 8) companions per 100 systems.

Since the pointed ROSAT observations were performed with different integration times, it is difficult to determine their luminosity limit. Therefore, and because of the small number of stars involved, we do not try to correct a possible detection bias of binaries found with pointed observations. However, we would like to point out that the multiplicity of our sample does not change significantly if we exclude all sources found with pointed observations.

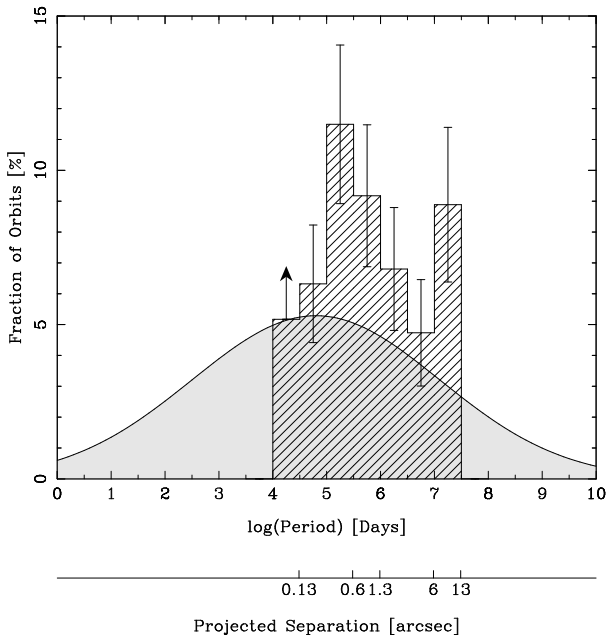

Fig. 5. Binary frequency as a function of orbital period, resp. separation. By binary frequency, we mean the number of companion stars with orbital period in a given interval divided by the total number of systems. This implies that triples are represented as two pairs. The histogram shows the combined results of Leinert et al. (1993) and this work; the shaded curve is the distribution of binaries among solar-type main-sequence stars (Duquennoy & Mayor 1991). The number of companions with periods between 10^4 and $10^{4.5}$ days is only a lower limit since it is difficult to resolve binaries with such a small separation. This is why we are certain we did not discover all of them

5. Discussion

5.1. Comparison of the young star samples before and after ROSAT

Optimum use can be made of the results of this study if we combine our results with those of Leinert et al. (1993) who surveyed the young stars in Taurus-Auriga known before ROSAT. Their sample includes 104 stars, 39 of which are binaries, 3 triples, and 2 quadruple stars, giving a total of 51 companions.

Before combining the two samples, we have to compare whether the two samples lead to similar results and simply can be added to increase the statistical accuracy, or whether they are so different that they have to be treated separately. The comparison in Table 4 shows that indeed the observed multiplicity in the two samples is similar and that they can well be combined for statistical purposes.

5.2. Pre-main-sequence vs. main-sequence stars

Now we are going to compare our data from the combined sample to the multiplicity survey of Duquennoy & Mayor (1991, DM91). Although other studies exist (e. g. Mayor et al. 1992; Fischer & Marcy 1992), this is not only the most comprehensive study, but also includes the spectral types most of our stars will have after evolution to the main sequence (F and G).

To do this comparison, we have to convert our measured angular separations into orbital periods. This is impossible for individual objects of our sample since the orbital parameters are not known. Instead, we use the same method as Leinert et al. (1993) and rely on statistical arguments. First, we convert the angular separation into a linear separation. To perform this, we use a distance to the Taurus star forming region of 140 pc (Elias 1978, Preibisch & Smith 1997). This choice is supported by new observations of the astrometry satellite Hipparcos, which measured the parallaxes of five T Tauri stars in Taurus, giving a weighted mean distance of 140 ± 14 pc (Wichmann et al. 1997).

The second step is to convert the projected separation into a semi-major axis, taking into account the probability for a binary to be observed in a particular position in its

orbit and the inclination of the orbital plane. These two effects lead to a combined reduction factor of 0.95 (see Leinert et al. 1993 for details). Finally, we use Kepler's third law with a system mass of $1\,M_\odot$ to compute the orbital periods. With these numbers, the separation range $0.13''$ to $13''$ transforms into a range of periods from $10^{4.5}$ to $10^{7.5}$ days.

Figure 5 shows the result of the comparison. The combined sample of Leinert et al. (1993) and this work contains 85 companions in 174 systems, corresponding to (48.9 ± 5.3) companions per 100 T Tauri stars. DM91 find (25.3 $\pm$ 3.9) companions per 100 main-sequence stars in the period interval covered by our survey. This means 100 T Tauri stars have (23.5$\pm$6.6) additional companions compared to solar-type main-sequence stars. In other words, the multiplicity of pre-main-sequence stars in Taurus is enhanced by a factor of 1.93 ± 0.26 ($3.6\,\sigma$).

DM91 claim to have detected all binaries down to mass ratios of 0.1. Our survey is complete for brightness ratios in K larger than 0.1 to about 0.01, depending on the separation. It is not obvious which relation should be used to convert the flux ratios of pre-main-sequence objects to mass ratios. A proportionality or near-proportionality of K brightness and mass for young stars has repeatedly been assumed and should be a good approximation for coeval binary components contracting along the Hayashi line (Simon et al. 1992, Zinnecker et al. 1992, Reipurth and Zinnecker 1993). As the stars contract down their evolutionary tracks, the relation between mass and the K luminosity for the lower main sequence, $L \propto M^{1.6\ldots2.5}$ (Henry & McCarthy 1993), should be approached. This means our survey is propably not as complete as that of DM91. Therefore, the enhancement factor of 1.93 is rather a lower limit. Furthermore, DM91 added a correction for companions undetected because of detection biases, while we prefer to use only the number of binaries we actually are able to see.

5.3. Classical vs. weak-line T Tauri stars

The combined sample of Leinert et al. (1993) and this work contains 72 classical and 102 weak-line T Tauri stars. This allows us to compare the multiplicity of these two types of T Tauri stars.

First, we compare the total numbers of binary orbits. We find 39 companions among the CTTS, or (54.2 ± 8.7) companions per 100 systems. Among the WTTS, we find 45 companions, corresponding to (44.1 ± 6.6) companions per 100 systems. The errors have been estimated by taking the square root of the number of companions. Within the errors, there is no systematic difference between classical and weak-line T Tauri stars.

Figure 6 shows the distributions of companions as a function of their orbital period separately for companions to CTTS and WTTS. We performed an χ^2 test, resulting

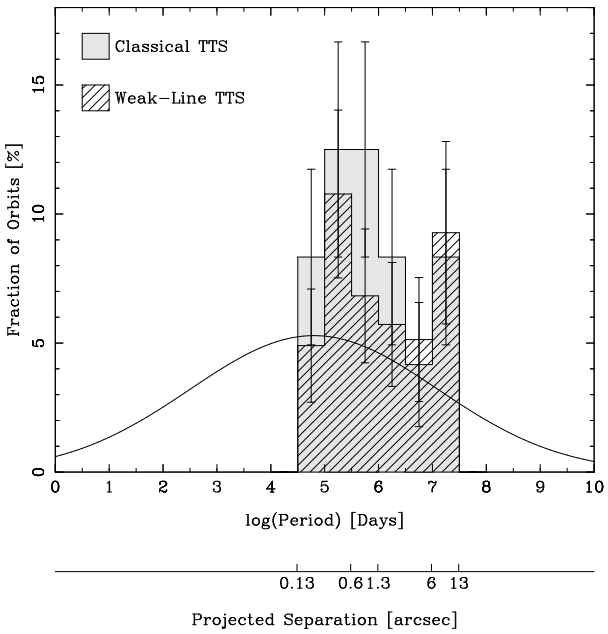

Fig. 6. Binary frequency as a function of orbital period, broken down into classical (shaded histogram) and weak-line T Tauri stars (lined histogram). The Gaussian curve denotes the distribution of binaries among solar-type main-sequence stars (Duquennoy & Mayor 1991)

in a reduced χ^2 of 0.66. If both samples were drawn from the same distribution, one would find larger values of χ^2 with a probability of 69 %. We take this as confirmation of the assumption that the distributions of CTTS and WTTS binaries are indeed essentially identical.

This is in contrast to the result of Ghez et al. (1993) who reported a difference in the distributions of WTTS and CTTS binary stars as a function of the separation: they find that the WTTS binary star distribution is enhanced at smaller separation (< 40 AU or $0.29''$) relative to the CTTS binary star distribution. Our data (Fig. 6) do not support their finding.

5.4. Surface density of companions

In a study of clustering of young stars in different star forming regions, Simon (1997) found that the differential surface density of companions Σ followed a power law $\Sigma(\theta) \propto \theta^{-b}$ as a function of the angular separation θ with the exponent b close to 2.0 in all three regions studied. Since our combined sample in Taurus is considerably larger than the sample based on lunar occultations used by Simon (1997), we recalculated the exponent for the surface density distribution on the basis of the enlarged sample. The resulting exponent ($b = -1.99 \pm 0.09$, see Fig. 7) is essentially the same as given by Simon (-2.01 ± 0.06). In descriptive terms, this means that in the log(period)/log(separation) diagram the distribution of companions is flat (because then $\mathrm{d}N/\mathrm{d}\theta \propto 1/\theta$ and

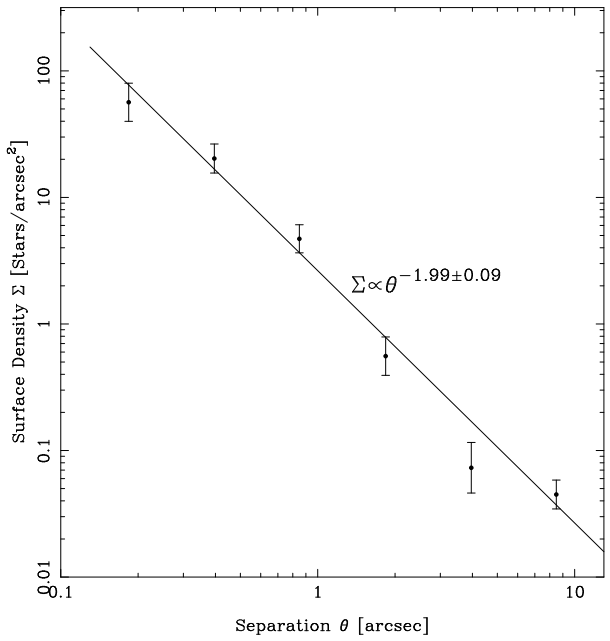

Fig. 7. Differential surface density of companions for the combined sample. To determine this, the separations have been binned in non-overlapping annular areas starting at 0.13″ and increasing by factors of $10^{1/3}$ until the outer limit 13″ is reached. The number of companions in each annulus divided by the area of the annulus gives the surface density shown. The straight line shows the best fit to the points

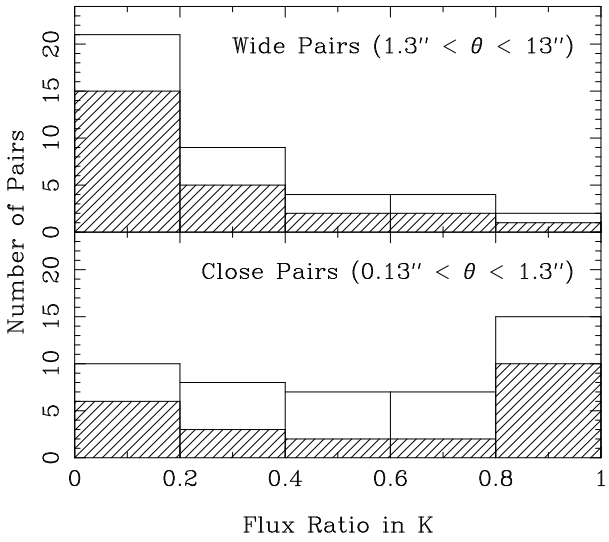

Fig. 8. Distribution of flux ratios for close companions (between 0.13″ and 1.3″ or 18 AU and 180 AU separated from the primary) and for distant companions (between 1.3″ and 13″ or 180 AU and 1800 AU from the primary). The hatched histogram shows the numbers of companions to WTTS, the open histogram those of companions to CTTS. The star 40C has been excluded here because we know it is probably a background star

the area of the annuli as a function of θ is proportional to θ). As far as the range of separations studied here is concerned, a flat distribution in $\mathrm{d}N/\mathrm{d}\log(\theta)$ apparently is consistent with the data and $\mathrm{d}N/\mathrm{d}\theta \propto \theta^{-1}$ is a reasonable first approximation for the separation distribution of companions to young stars in Taurus.

5.5. Is there a difference between close and wide companions?

In Fig. 8 we plot the distribution of flux ratios for the companions in the ROSAT-selected sample and the sample of Leinert et al. (1993), split into close pairs with the companion separated 0.13″ to 1.3″ (18 AU – 180 AU) from their primary and wide pairs with companions separated 1.3″ to 13″ (180 AU – 1800 AU). The dividing line has been set somewhat arbitrarily at what we consider is a typical accretion disk radius ($\approx$ 150 – 200 AU, or 1.1" – 1.5"). In triple systems, we use the ratio of the combined flux of the inner pair to the flux of the third component as flux ratio of the outer pair.

The distributions for close and wide pairs are not identical: the wide binaries preferentially have small flux ratios, while the distribution of close pairs is flat with a possible slight increase towards equal flux ratios. A χ^2 test for the combined sample yields a probability of only 1 % that the two samples have been drawn from the same distribution. The histogram of wide pairs still contains three background stars, however, we do not know their flux ratios (one background star has already been excluded since we know that the star 40C is one). If we subtract these three background stars from the bin for flux ratios between 0.0 and 0.2, we get a probability of 2.4 %. We take this as indication that there is a difference between the brightness ratios in close and wide pairs.

On the other hand, one can argue that the difference at the lowest brightness ratios simply reflects our inability to detect faint companions close to the primary. We certainly admit that we may have missed some companions with these properties. But we note that making the difference in the lowest brightness ratio bin disappear would require adding about 10 unseen companions, i. e. would require to double the number of companions. It therefore seems unlikely to us that the difference at the lowest brightness ratios is caused by the above-mentioned bias. Nevertheless, in order to not have to consider this bias at all, we also performed a χ^2 test for the upper four bins only, negelecting the bin with the lowest brightness ratios. The result is a probability of still only 16 % that the two distributions are identical. This maintains our conclusions that there is a difference between the brightness ratio distributions of close and wide pairs.

If we take the flux ratios in K as an approximation for the mass ratios, then our findings match the prediction of the model calculations of Bate and Bonnell (Bate 1997, Bate & Bonnell 1997). They studied accretion from a collapsing cloud onto a protobinary at its center. For a

close system, the infalling material has comparatively high angular momentum, which leads to accretion onto the secondary and therefore drives the mass ratio to higher values. For a wide binary system, the opposite is true, and in the outcome such long-period systems are more likely to have small mass ratios. However, mass outflows are not considered in their models. These may change the results significantly.

As we already mentioned in Sect. 5.2, the relation between mass and the K luminosity for our pre-main-sequence stars is somewhere between $L \propto M$ and $L \propto M^{1.6\ldots2.5}$. The latter relation would distort the scale of the abscissa in Fig. 8, but not alter the result. In classical T Tauri stars, the contribution to the K brightness from an accretion disk is non-negligible and may be strong. Probably, this effect would smear out intrinsic differences in the brightness ratios of the stars alone and not mimic them. This could explain why the difference between close and wide pairs is more clearly observed in the weak-line T Tauri stars. Therefore, we still accept that the difference we see in the brightness ratios translates into a difference in the mass ratio distribution for close and wide pairs.

5.6. Consequences of the controversy on the age of ROSAT-selected stars

Briceño et al. (1997) claim that the majority of ROSAT-detected sources are not pre-main-sequence objects, but $\approx 10^8$ years old, essentially zero-age main-sequence stars. We are not going to contribute to this discussion. In particular, we hesitate to use the binary frequency to determine the age of a stellar group; this would be premature and questionable: multiplicity may depend on several parameters, and none of these possible relations has been firmly established so far, Therefore, our measurement of the binary frequency can not answer the question about the status of these stars. Instead, we will show that it does not weaken our conclusions if the stars have already reached the main sequence.

For the purpose of this discussion we assume with Briceño et al. (1997) that a sizeable fraction of the ROSAT-detected sources are about 10^8 years old and not certainly associated with the Taurus clouds. There would be nothing to discuss if all of these sources belonged to Taurus, and there is sufficient evidence for young WTTS in Taurus to reject the possibility that *all* ROSAT-detected sources could be zero-age main-sequence objects. To study the influence which a different age of a fraction of the stars would have on our multiplicity survey, we consider two limiting cases: either the multiplicity of the zero-age main-sequence stars is as high as that of the pre-main-sequence stars in Taurus, or it is similar to that of the main-sequence stars surveyed by Duquennoy and Mayor (1991).

The first case leads to the conclusion that there is no evolution of multiplicity while the stars evolve from their pre-main-sequence phase to the main-sequence. This would only emphasize the discrepancy in multiplicity, making it a discrepancy between different groups of stars on the main sequence. The prediction of Briceño et al. (1997) that the 10^8-year-old stars are somewhat nearer to us than the Taurus star forming region (100 – 120 pc instead of 140 pc) is not important in this respect. Even changing the distance by a factor of 2 would shift the histogram in Fig. 5 by only one bin. A high binary frequency among zero-age main-sequence stars would be in remarkable contrast to the findings of Bouvier et al. (1997), who have searched for binaries among G and K dwarf members of the Pleiades cluster, which are also about 10^8 years old. They derive a multiplicity similar to that of main-sequence stars. The way out of this discrepancy between stars of similar age could be given by the hypothesis that the local environment has a decisive influence on the binary frequency.

In the second case, if the multiplicity of the old stars in our sample is the same as on the main sequence, there have to be even more binaries and multiples among the ROSAT-selected pre-main-sequence objects in order to yield the high multiplicity we observe in the full ROSAT-selected sample. If, for example, half of the ROSAT-selected sample showed the multiplicity properties of main-sequence stars, the remaining 37 young stars would need to have 25 companions in the range of separations 0.13" – 13", almost three times the value found on the main sequence.

If we assume that the majority of the ROSAT-selected stars are indeed zero-age main-sequence stars, then the question of how to explain the differences in multiplicity between ROSAT-selected and main-sequence stars would only be rendered more difficult, however necessary and interesting the discussion on the age of these stars may be.

6. Summary and conclusions

We have searched a sample of 75 X-ray selected T Tauri stars in the Taurus star forming region for duplicity. We find

— the same multiplicity in this sample as was discovered in an earlier study of 104 differently selected young stars in Taurus by Leinert et al. (1993),
— no systematic difference in the multiplicity of classical and weak-line T Tauri stars (within the combination of the two samples),
— an excess of duplicity in the combined sample over the duplicity of solar-type main-sequence stars by a factor of 1.93 ± 0.26 ($3.6\,\sigma$),
— an indication that close companions have a flat brightness ratio distribution with a tendency towards equal brightnesses, while wide binaries preferentially have low brightness ratios.

We conclude that the discrepancy between the multiplicity of pre-main-sequence and main-sequence stars cannot be

resolved by the large numbers of the presumably older WTTS in young associations like Taurus. This conclusion only gets stronger if a significant fraction of the ROSAT-selected stars are not pre-main-sequence objects but about 10^8 yrs old as proposed by Briceño et al. (1997).

The simplest explanation for the overabundance of binaries in Taurus-Auriga is the hypothesis that more binaries form there than on average in other star forming regions. This means that either Taurus-Auriga itself or all T associations are a special case. This would be in line with the suggestion by Durisen & Sterzik (1994) that more binaries may form in low-temperature clouds. The findings of Simon et al. (1995) and Brandner et al. (1996) also support this hypothesis. They derive a binary frequency in the higher temperature star forming regions Ophiuchus and Scorpius-Centaurus that is nearly in agreement with that of main-sequence stars (enhanced by a factor of only 1.1 ± 0.3 in the case of Ophiuchus).

Another possible explanation would be the disruption of binary systems in embedded clusters (Kroupa 1995), if most stars form there . To test these hypotheses, it is necessary to perform similar multiplicity surveys in other star forming regions. Several of those surveys are underway or in preparation.

Acknowledgements. The authors would like to thank the MAGIC team for their assistance and ongoing support in using this nice camera. We also thank Rainer Wichmann for many helpful informations about "his" stars, and Mike Simon, Michael R. Meyer, and Pavel Kroupa for some useful suggestions. We are grateful to William Hartkopf for providing up-to-date orbits and ephemerides for several visual binaries used for plate-scale calibration.

References

Bate M.R., 1997, MNRAS 285, 16
Bate M.R., Bonnell I.A., 1997, MNRAS 285, 33
Bouvier J., Rigaut F., Nadeau D., 1997, A&A 323, 139
Brandner W., Alcalá J. M., Kunkel M., Moneti A., Zinnecker H., 1996, A&A 307, 121
Briceño C., Hartmann L.W., Stauffer J.R., Gagné M., Stern R.A., Caillault J.-P., 1997, AJ 113, 740
Duquennoy A., Mayor M., 1991, A&A 248, 485
Durisen R.H., Sterzik M.F., 1994, A&aA 286, 84
Elias J. H., 1978, ApJ 224, 857
Fischer D. A., Marcy G. W., 1992, ApJ 396, 178
Ghez A.M., Neugebauer G., Matthews K., 1993, AJ 106, 2005
Ghez A., McCarthy D.W., Patience J., Beck T., 1997, ApJ 481, 378
Henry T.J., McCarthy D.W., 1993, AJ 106, 773
Herbst T.M., Birk C., Beckwith S.V.W., Hippler S., McCaughrean M.J., Mannucci F., Wolf J., 1993, Proc. SPIE 1946, Fowler, A.M. (ed.), p. 605
Knox K.T., Thompson B.J., 1974, ApJ 193, L45
Kroupa P., 1995, MNRAS 277, 1491
Lada, J.L., and Lada, E.A., 1991, in: The Formation and Evolution of Star Clusters, Janes, K. (ed.), Astron. Soc. Pac. Conf. Series 13, p. 3
Leinert Ch., Zinnecker H., Weitzel N., Christou J., Ridgeway S.T., Jameson R., Haas M., Lenzen R., 1993, A&A 278, 129
Leinert, Ch., Henry, T., Glindemann, A., McCarthy, D.W., 1996, A&A, in press
Lohmann A.W., Weigelt G., Wirnitzer B., 1983, Appl. Opt., 22, 4028
Mayor M., Duquennoy A., Halbwachs J.-L., Mermilliod J.-C., 1992, In: Complementary Approaches to Double and Multiple Star Research, McAlister, H.A., Hartkopf, W.I. (eds.), IAU Colloquium 135, San Francisco, p. 73
Miller G.E., Scalo J.M., 1978, PASP 90, 506
Neuhäuser R., Sterzik M.F., Schmitt J.H.M.M., Wichmann R., Krautter J., 1995, A&A 295, L5
Petr M.G., Coudé du Foresto V., Beckwith S.V.W., Richichi A., McCaughrean M.J., 1998, ApJ, submitted
Preibisch T., Smith M. D., 1997, A&A 322, 825
Prosser C.F., Stauffer J.R., Hartmann L., Soderblom D.R., Jones B.F., Werner M.W., McCaughrean M.J., 1994, ApJ 421, 517
Reipurth B., Zinnecker H., 1993, A&A 278, 81
Richichi A., Leinert Ch., Jameson R., Zinnecker H., 1994, A&A 287, 145
Simon M., Chen W.P., Howell R.R., Benson J.A., Slowik D., 1992, ApJ 384, 212
Simon M., Ghez A.M., Leinert Ch., Cassar L., Chen W.P., Howell R.R., Jameson R.F., Matthews K., Neugebauer G., Richichi A., 1995, ApJ 443, 625
Simon M., 1997, ApJ 482, L81
Ungerechts H., Thaddeus P., 1987, Ap. J. Suppl. 63, 645
Walter F.M., Brown A., Mathieu R.D., Myers P.C., Vrba F.J., 1988, AJ 96, 297
Wichmann R., Krautter J., Schmitt J.H.M.M., Neuhäuser R., Alcalá J.M., Zinnecker H., Wagner R.M., Mundt R., Sterzik M.F., 1996, A&A 312, 439
Wichmann R., Bastian U., Krautter J., Jankovics I., Rucinski S.M., 1997, In: Proceedings of the HIPPARCOS Venice '97 Symposium, Perryman M.A.C., Bernacca P.L. (eds.), ESA SP-402
Zinnecker H., Brandner W., Reipurth B., 1992, In: Complementary Approaches to Double and Multiple Star Research, McAlister, H.A., Hartkopf, W.I. (eds.), IAU Colloquium 135, San Francisco, p. 50